# Wnt signaling regulates neural plate patterning in distinct temporal phases with dynamic transcriptional outputs

**David G. Green**[a,1], **Amy E. Whitener**[b,2], **Saurav Mohanty**[a], **Brandon Mistretta**[a], **Preethi Gunaratne**[a], **Alvin T. Yeh**[c], **Arne C. Lekven**[a,*]

[a]Department of Biology and Biochemistry, University of Houston, Houston, TX, 77204-5001, USA

[b]Department of Biology, Texas A&M University, College Station, TX, 77843-3258, USA

[c]Department of Biomedical Engineering, Texas A&M University, College Station, TX, 77843-3120, USA

## Abstract

The process that partitions the nascent vertebrate central nervous system into forebrain, midbrain, hindbrain, and spinal cord after neural induction is of fundamental interest in developmental biology, and is known to be dependent on Wnt/β-catenin signaling at multiple steps. Neural induction specifies neural ectoderm with forebrain character that is subsequently posteriorized by graded Wnt signaling: embryological and mutant analyses have shown that progressively higher levels of Wnt signaling induce progressively more posterior fates. However, the mechanistic link between Wnt signaling and the molecular subdivision of the neural ectoderm into distinct domains in the anteroposterior (AP) axis is still not clear. To better understand how Wnt mediates neural AP patterning, we performed a temporal dissection of neural patterning in response to manipulations of Wnt signaling in zebrafish. We show that Wnt-mediated neural patterning in zebrafish can be divided into three phases: (I) a primary AP patterning phase, which occurs during gastrulation, (II) a mes/r1 (mesencephalon-rhombomere 1) specification and refinement phase, which occurs immediately after gastrulation, and (III) a midbrain-hindbrain boundary (MHB) morphogenesis phase, which occurs during segmentation stages. A major outcome of these Wnt signaling phases is the specification of the major compartment divisions of the developing brain: first the MHB, then the diencephalic-mesencephalic boundary (DMB). The specification of these lineage divisions depends upon the dynamic changes of gene transcription in response to Wnt signaling, which we show primarily involves transcriptional repression or indirect activation. We show that *otx2b* is directly repressed by Wnt signaling during primary AP patterning, but becomes resistant to Wnt-mediated repression during late gastrulation. Also during late gastrulation, Wnt signaling becomes both necessary and sufficient for expression of *wnt8b, en2a*, and *her5* in mes/r1. We suggest that the change in *otx2b* response to Wnt regulation enables a transition to the mes/r1 phase of Wnt-mediated patterning, as it ensures that Wnts expressed in the midbrain and

---

[*]Corresponding author. alekven@uh.edu (A.C. Lekven).
[1]Current address: Department of Cell and Systems Biology, University of Toronto, 25 Harbord Street, Ramsey Wright Room 603, Toronto, ON, Canada, M5S3G5.
[2]Current address: Vanderbilt Eye Institute Reseach Laboratories, 1161 21st Ave S, AA7100MCN, Nashville, TN 37232.

MHB do not suppress midbrain identity, and consequently reinforce formation of the DMB. These findings integrate important temporal elements into our spatial understanding of Wnt-mediated neural patterning and may serve as an important basis for a better understanding of neural patterning defects that have implications in human health.

## Keywords

Vertebrate; Neural plate; Anterior posterior patterning; Wnt; Zebrafish; Mes/r1; otx2; Midbrain-hindbrain boundary; RNA-Seq

## 1. Introduction

The vertebrate central nervous system is partitioned along the anteroposterior (AP) axis into four gross divisions-forebrain, midbrain, hindbrain, and spinal cord– in a progressive process that initiates concurrently with, or immediately after, neural induction in the early gastrula (Green et al., 2015). The mechanism by which the neural plate is patterned along the AP axis has been of interest for over 50 years, with the prevailing model being the "activation-transformation" model proposed by Nieuwkoop (1952). This hypothesis states that neural induction specifies neural ectoderm with anterior character (i.e. forebrain) that is subsequently "posteriorized" (i.e. induction of midbrain, hindbrain, and spinal cord) by signals emanating from paraxial mesoderm at the posterior aspect of the neural plate that influence cell fate in a graded fashion. While evidence has amassed that is consistent with this hypothesis (Cox and Hemmati-Brivanlou, 1995; Durston et al., 1989; Kiecker and Niehrs, 2001; McGrew et al., 1995, 1997; Nordstrom et al., 2002) , recent findings have challenged the view of a simple anterior to posterior signaling gradient being interpreted into anterior-posterior domains. For example, recent evidence has suggested that cells may be biased towards specific fates along the anteroposterior axis prior to neural induction (Metzis et al., 2018), and that spinal cord fate is induced via a distinct signaling mechanism from other CNS territories (Polevoy et al., 2019).

Despite challenges to the activation-transformation model, considerable evidence clearly implicates Wnt, Fgf, and retinoic acid (RA) signaling in the mechanism of neural plate AP patterning, and, of these, Wnt signaling levels are capable of inducing neural AP fates according to concentration (Kiecker and Niehrs, 2001; Nordstrom et al., 2002; for reviews see Elkouby and Frank, 2010; Gibbs et al., 2017). However, exactly when these signals are interpreted by the neural plate to establish the AP axis is less clear. For example, Wnt ligands expressed in paraxial mesoderm progenitors impart polarity on the newly induced neural ectoderm by specifying posterior identity, a process termed "neural posteriorization" (Green et al., 2015). In zebrafish, this function is attributed to Wnt8a (Erter et al., 2001; Lekven et al., 2001; Rhinn et al., 2005). *wnt8a* expression is initiated in the embryonic margin prior to neural induction and remains present throughout epiboly (Kelly et al., 1995; Lekven et al., 2001). While *wnt8a* expression is maintained in the margin during epiboly, it is unclear if it serves a functional role in neural posteriorization throughout epiboly or only during a discrete portion of epiboly. Further confusing the issue is the fact that several neural AP patterning steps involving Wnt signaling are activated downstream of *wnt8a*. For

instance, expression of Wnt8b in the diencephalon, which, together with the Wnt antagonist Tlc, patterns the telencephalon, is altered by changes to Wnt8a signaling (Houart et al., 2002). In addition to activating downstream effectors, Wnt8a also directly patterns the neural plate AP axis by determining the position of the interface between otx2-expressing mesencephalic progenitors and *gbx*-expressing hindbrain progenitors (Rhinn et al., 2005, 2009). The *otx/gbx* interface position determines the future site of the midbrain hindbrain boundary (MHB), a lineage restriction border located within a conserved physical constriction of the neural tube (Joyner et al., 2000; Langenberg and Brand, 2005; Matsuo et al., 1995; Millet et al., 1999). Wnt signaling is also necessary for specification of mes/r1, the neural domain comprising mesencephalon (mes) and the anterior hindbrain (r1) within which the MHB forms (McMahon and Bradley, 1990; Thomas and Capecchi, 1990; Zervas et al., 2004). Subsequently, Wnt signaling is initiated in the MHB and integrated into the MHB gene regulatory network (Buckles et al., 2004; Lekven et al., 2003). It is unclear if these different sources of Wnt signaling pattern the neural plate in distinct temporal phases or if they signal at the same time, but with different outputs, such as through the activation of different downstream receptors (Kim et al., 2002; Momoi et al., 2003).

How Wnt-mediated posteriorization is mechanistically linked to the specification of cell fates in the neural plate is also not well understood. While there is significant evidence that Wnt signaling can suppress anterior neural markers and induce posterior markers (Kudoh et al., 2002), many of these experiments have been performed in explants, which may not completely recapitulate specific developmental contexts (Kiecker and Niehrs, 2001; Nordstrom et al., 2002). As recent single-cell RNA-seq methodologies have revealed unexpected transcriptional diversity among cells of a presumed restricted lineage (Farrell et al., 2018; Raj et al., 2018), it is likely that much is unknown about the timeline from Wnt signal reception by neural plate cells to transcriptional changes underlying AP-specific fate.

We present evidence that the response of the neural ectoderm to Wnt signaling can be divided into three distinct phases. First is the primary AP patterning phase, when Wnt8a signals across the neural plate AP axis to determine the allocation of progenitor cells to anteroposterior fate domains. The signaling events that occur here are interpreted by the neural plate initially as transcriptional changes in a relatively small number of genes, some directly repressed by Wnt, that ultimately lead to patterning shifts in the AP axis that take several hours to unfold. Second is the mes/r1 phase, during which Wnt ligand expression is maintained in mes/r1 through a feedback network that maintains midbrain identity and the MHB gene regulatory network. Third is the MHB morphogenesis phase, during which Wnt signaling plays a role in maintaining MHB gene expression and constriction morphogenesis, but no longer impacts the AP pattern of the brain. These findings provide a temporal framework in which we describe Wnt-mediated neural patterning, and show that both ligand availability as well as competency of different regions of the neural ectoderm are dynamic and essential for the establishment of neural patterning in the AP axis.

## 2.  Materials and methods

### 2.1.  Zebrafish care

Zebrafish were maintained as described (Westerfield, 2000). AB, TL, and AB-TL hybrid strains serve as our wild-type stocks. The University of Houston and Texas A&M University Institutional Animal Care and Use Committees approved vertebrate animal procedures. The *Tg(hsp70l:dkk1b-GFP)$^{w32Tg}$* and *Tg(hsp70l:wnt8a-GFP)$^{w34Tg}$* lines were a kind gift from Dr. Randall Moon (University of Washington) (Stoick-Cooper et al., 2007; Weidinger et al., 2005).

### 2.2.  Heat shocks and in situ hybridizations

*Tg(hsp70l:dkk1b-GFP)$^{w32Tg}$* (hereafter referred to as *hs:dkk1b*/+) were crossed to wild-type fish, and embryos were collected within 15 min of spawning. Heat shocks were performed by placing groups of 10 embryos in standard fish water (zfin.org) into PCR tubes, incubating at 37°C for 60 min, then returning embryos to 29°C for recovery to the designated stages. *Tg(hsp70l:wnt8a-GFP)$^{w34Tg}$* (hereafter, *hs:wnt8a/+*) were crossed to wild-type fish, and embryos were collected and heat shocked in groups of 10 in PCR tubes at 39 °C for 30 min, then returned to 29 °C for recovery to the designated stage. Embryos were fixed in 4% paraformaldehyde overnight at 4 °C. Unless otherwise indicated, heat shock transgenic embryos were unambiguously identified after heat shock by morphological or gene expression criteria and represented ~50% of offspring. All experiments were performed at least twice, with a minimum of 25 embryos in each group. In situ hybridizations were performed as described previously (Ramel et al., 2004). Embryos were imaged with a Nikon SMZ745T or a Nikon SMZ25. Figures were assembled with Adobe Photoshop CC. Brightness and contrast were adjusted for clarity.

### 2.3.  Drug treatments

Wild-type embryos were collected within 15 min of spawning. BIO (Sigma) was dissolved in DMSO to make a stock concentration of 10 mM. The BIO stock solution was diluted to 10 μM in fish water for incubations. 15 embryos were placed in each well of a 9 well plate and incubated in 1 ml of 10 μM BIO for 30 min. Embryos were subsequently washed three times in fish water and grown to the designated stage at 29 °C. Drug treatments were performed in triplicate, with n  30 embryos in each group.

Cycloheximide (CHX; Sigma) was dissolved in ETOH to a stock concentration of 10 mg/ml. The CHX ETOH stock solution was then diluted in fish water to 10 μg/ml for incubations. The efficacy of CHX was tested by treating *hs:dkk1b*/+ embryos with 10μg/ml CHX and heat shocking embryos for 60 min at 37 °C. In untreated samples, 50% of embryos showed GFP fluorescence within 2 h; CHX treated embryos did not show any GFP fluorescence (not shown). For treatments, 15 embryos were placed in each well of a 9 well plate with either 1 ml of 10 μg/ml CHX or 1 ml of 10 μg/ml CHX & 10 μM BIO. Controls were incubated in either 0.1% ETOH, 0.1% DMSO or a combination of the two. Embryos were kept in CHX from the designated stage until bud stage (10 hpf). Embryos were treated with 10 μM BIO/CHX for 30 min, then washed in 10 μg/ml CHX three times and shifted to 10 μg/ml CHX until bud stage.

### 2.4.   RNA-sequencing transcriptome analysis

*hs:dkk1b*/+ or *hs:wnt8a*/+ embryos, identified by fluorescence, and their wild-type siblings were collected from multiple mating fish pairs, then embryos at the desired time points were immediately homogenized in Trizol (Sigma). For each sample, n = 30 embryos, with three biological replicates for each condition. Total RNA was isolated with Direct-zol RNA kits (Zymo, Inc.), and was given to the Texas A&M AgriLife Research Genomics and Bioinformatics Service for library preparation and Illumina sequencing. The RNA-seq raw fastq data was processed with CLC Genomics Workbench 12 (Qiagen). The Illumina sequencing adaptors were trimmed and reads were mapped to GRCz11 zebrafish reference genome. Read alignment was represented as integer counts by using parameters of mismatch cost 2, insertion cost 3, deletion cost 3, length fraction 0.8, similarity fraction 0.8, max of 10 hits for a read. Integer read counts were normalized by Trimmed Means of M-values (TMM) algorithm. After normalization, we performed differential gene expression using the EdgeR package (Robinson and Oshlack, 2010) which uses a generalized linear model linked to the negative binomial distribution to identify significance. The significance level of FDR adjusted *p*-value of 0.05 was used to identify differentially expressed genes.

## 3.   Results

### 3.1.   Temporal regulation of canonical Wnt signaling by inducible transgenes

To dissect stage-specific effects of Wnt signals on neural AP patterning, we took advantage of zebrafish transgenic lines bearing either a heat shock inducible Wnt antagonist (*Tg(hsp70L:dkk1b-GFP)$^{w32Tg}$*) or agonist (*Tg(hsp70L:wnt8a-GFP)$^{w34Tg}$*) transgene. Dkk1b blocks canonical Wnt signaling by binding the essential co-receptor Lrp5/6 (Ahn et al., 2011), while Wnt8a can activate the canonical Wnt pathway through multiple Frizzled receptors (Hsieh et al., 1999). Both transgenes are induced globally with heat shocks. We crossed transgenic adults (hereafter referred to as *hs:dkk1b*/+ or *hs:wnt8a*/+) with wild-type adults and heat shocked offspring embryos at specific developmental intervals, with wild-type sibling embryos from each clutch serving as the control. Because the duration of Wnt antagonism or overexpression after standard heat shock regimens in these lines had not been previously well characterized, we assayed the transcript dynamics of *dkk1b* or *wnt8a* and the Wnt response gene, *axin2* in heat shocked transgenic embryos (Fig. S1). With *hs:dkk1b*/+, *dkk1b* transcripts are present at high levels at 1 h post heat shock and remain high until 2 h post heat shock, after which expression begins to decline; at 5 h post heat shock, elevated *dkk1b* is no longer detectable (Figs. S1A–E, and data not shown). This pattern correlates with the observed pattern of *axin2*, a commonly used measure of Wnt/β-catenin activity (Jho et al., 2002). By 1 h post heat shock, *axin2* levels are strongly reduced and remain low until 4 h post heat shock (Figs. S1F–I). By 5 h post heat shock, *axin2* levels are not noticeably different from wild-type (Fig S1J). From these data, we deduce that a 1h heat shock pulse interferes with Wnt signaling for a duration of ~4 h after the heat shock, with recovery by 5 h post heat shock. Thus, we deduce a span of 6 h from the beginning of the heat shock to the end of suppression of canonical Wnt signaling (Fig. S2). In a similar analysis of Wnt pathway activation by *hs:wnt8a*/+, we found that a 0.5 h heat shock pulse leads to an induction of the *wnt8a-gfp* transgene and *axin2* by 0.5 hph (Fig. S1K–M,O–Q), with a return to normal expression levels between 1.0-1.5 hph (Figs. S1N and R). Thus, we deduce a span

of 2 h from the beginning of the heat shock to the end of activation of canonical Wnt signaling (Fig. 4).

## 3.2. Timed Wnt loss-of-function defines three distinct functional periods for Wnt mediated neural plate patterning

To determine whether neural plate development involves temporally distinct requirements for Wnt signaling, *hs:dkk1b*/+ was induced at ten time points during the first 24 h of development, spanning gastrulation through segmentation stages (Fig. S2). These treatments produced four clearly distinguishable phenotypic categories at 27 h post fertilization (hpf) that correlate with time of heat shock (Fig. 1 and Fig. S2, and data not shown). Wnt antagonism at 3 hpf produces strongly dorsoanteriorized embryos falling into the C3–C5 dorsalization classes (Kishimoto et al., 1997)(Fig. 1B), thus recapitulating the previously described *wnt8a* loss of function phenotype (Baker et al., 2010; Hino et al., 2018; Lekven et al., 2001). Initiating Wnt antagonism at 4.7 hpf (30% epiboly stage) results in axis truncation, abnormal brain morphology, and enlarged eyes, reflective of neural anteriorization, but not dorsalization (Fig. 1C). Wnt antagonism at 7 hpf (70% epiboly) results in greatly abnormal brain morphology including the loss of midbrain and MHB with minor body truncation (Fig. 1D). Antagonism at 11 hpf results in significantly less severe brain malformations that include MHB absence (Fig. 1E). Antagonism at 14 hpf results in a reduction in the MHB constriction, though brain morphology appears otherwise normal (Fig. 1F). Heat shock at 16 hpf produced no visible morphological defects (Fig. 1G).

To complement our morphological assessment, we assayed forebrain, midbrain, MHB, and hindbrain cell populations by *in-situ* hybridization. Initiation of Wnt antagonism at 3 or 4.7 hpf led to global brain patterning defects, including posterior shifts in forebrain domains (e.g. enlarged $epha4a^-$ telencephalon, posterior shift of $epha4a^+$ diencephalic expression domain, Fig. 1I,J), reduced midbrain (e.g. reduced distance between diencephalic and r1 $epha4a^+$ domains, Fig. 1J) and mild effects on hindbrain, though MHB gene expression appeared normal (e.g. *fgf8a* and *pax2a* MHB domains, Fig. 1P,Q,W,X). The severe morphological phenotype observed after initiating Wnt antagonism at 7 hpf reflected disrupted midbrain formation (indicated by continuity between diencephalic and r1 *epha4a* expression, Fig. 1K, arrowhead), and failure of MHB gene regulatory network maintenance (GRN) (loss of MHB *fgf8a* and *pax2a*, Fig. 1R,Y). The weaker phenotype observed after initiating Wnt antagonism at 11 hpf reflected a less affected midbrain domain (indicated by the restoration of gap between diencephalic and r1 *epha4a* domains, Fig. 1L,M, arrowhead), though the MHB GRN is still disrupted (Fig. 1S,Z). Initiating Wnt inhibition at 14 hpf resulted in largely normal neural patterning (Fig. 1M,T,A'), though the very shallow midbrain constriction is accompanied by the absence or severe reduction of MHB *pax2a* and *fgf8a* expression (Fig. 1F,inset,T,A'). Heat shock initiation at 16 hpf or later resulted in normal patterning (Fig. 1G,N,U,B').

By synthesizing the morphological and molecular analysis of these loss-of-function phenotypes with our data on the duration of Wnt inhibition associated with our *hs:dkk1b* regimen (and some uncertainty about the end of Wnt antagonism in our heat shock regimen), we deduce three distinct phases during which Wnt/β-catenin signaling influences neural

plate patterning (Fig. S2). The first phase, termed primary AP patterning, occurs during ~4-9.5 hpf (most of gastrulation), and corresponds to the transformation portion of Nieuwkoop's activation-transformation model. The second phase, the mes/r1 phase, occurs between ~9.5-12 hpf (early segmentation), and reflects a requirement for Wnt signaling for midbrain and MHB fate. The third phase, MHB morphogenesis, occurs between ~12-17 hpf (segmentation) and reflects dependence of the MHB gene regulatory network and MHB morphogenesis on Wnt/β-catenin signaling.

While this analysis identifies discrete phases for Wnt control of gross neural plate patterning, the 27 hpf phenotype may represent compounded effects of multiple earlier mis-patterning events. We therefore next assessed the phenotypic progression after our heat shock regimens. For phase one, we heat shocked *hs:dkk1b*/+ embryos at 4.7 hpf, then assayed *fgf8a, pax2a*, and *otx2b* expression at 9 and 10.5 hpf (Fig. 2). At 9 hpf, expression of both *fgf8a* and *pax2a* in the presumptive midbrain and hindbrain is absent (Fig. 2B,F, arrows), while *otx2b* expression is expanded posteriorly (Fig. 2J). However, by 10.5 hpf, *pax2a* and *fgf8a* expression is largely recovered (Fig. 2D,H), though *otx2b* expression remains somewhat expanded (Fig. 2L). This suggests an initial loss or delay of midbrain and hindbrain specification that subsequently recovers. Because 10.5 hpf is outside the window of Wnt antagonism in this experiment, recovery of *pax2a* and *fgf8a* expression could be through either Wnt signaling or an alternate mechanism.

To address the phenotypic progression after Wnt antagonism in phase two, we heat shocked embryos at 7 hpf, then examined *fgf8a, pax2a, en2a* and *wnt1* expression at 10.5, 14, and 16.5 hpf (Fig. 3). At 10.5 hpf, *pax2a* and *fgf8a* expression in the presumptive midbrain and hindbrain appear relatively normal (Fig. 3B,H), but both *en2a* and *wnt1* are substantially reduced or absent (Fig. 3N,T). By 14 hpf, *en2a* is absent, while MHB expression of *fgf8a*, *pax2a* and *wnt1* is lost, accompanied by the posterior expansion of telencephalic *fgf8a* and optic stalk expression of *pax2a* (Fig. 3D,J,P,V). By 16.5 hpf, telencephalic *fgf8a* is expanded slightly further posteriorly, and optic stalk *pax2a* expression extends to the prospective hindbrain domain (Fig. 3F,L). Hindbrain and dorsal neural tube *wnt1* expression persists at 14 and 16.5 hpf (Fig. 3V,X). Thus, in contrast to the secondary recovery observed after Wnt suppression in phase one, disruption of Wnt signaling in phase two results in the rapid loss of *en2a* and *wnt1* expression, followed by the progressive expansion of telencephalon and optic stalk to supplant midbrain and MHB territory.

To address phase three, we heat shocked *hs:dkk1b*/+ embryos at 14 hpf, then examined *wnt1, pax2a* and *fgf8a* expression at 17 and 19 hpf. In all cases, changes in gene expression at 17 and 19 hpf were difficult to observe by in situ hybridization, suggesting that the loss of expression of these genes in *hs:dkk1b*/+ embryos occurs between 19 and 27 hpf (Fig. S3, and data not shown). The significant delay in downregulation of MHB genes in this experiment may explain the lack of observed midbrain patterning defects compared to those observed with the earlier heat shocks. Thus, Wnt signaling is required during phase three for maintenance of MHB gene expression and normal formation of the MHB constriction, but midbrain tissue formation does not require Wnt signaling during this period.

In summary, our Wnt loss-of-function experiments identify discrete time limits to three independent phases of Wnt pathway influence on gross brain patterning: phase one comprises global AP patterning, phase two comprises mes/r1 maintenance, and phase three comprises MHB morphogenesis (Fig. S2). Phase one, limited to gastrula stages, corresponds to the transformation portion of the activation-transformation AP patterning model, which raises the question of whether AP patterning regulation by Wnt signaling could be attributed to signaling duration rather than signal levels per se. Additionally, in light of our previous results that forebrain, midbrain, and hindbrain domains respond differently to elevated Wnt8a signaling caused by increased mRNA stability (Wylie et al., 2014), we addressed whether AP fate domains might respond differently to timed Wnt pulses.

### 3.3. A Wnt overexpression assay identifies dynamic transcriptional control of otx2b by Wnt signaling

To complement the loss-of-function experiments and to test whether AP brain domains show temporally different responses to Wnt, we assayed the effects of timed Wnt overexpression with a particular focus on phase one, primary AP patterning. We globally activated canonical Wnt signaling by performing heat shocks on *hs:wnt8a*/+ and sibling +/+ embryos at four time points during epiboly and assayed brain divisions at 27 hpf (Fig. 4). Overexpression at all time points suppressed eye formation, indicative of a loss of forebrain fate. Consistent with this, the telencephalic expression domain of *zic1* is absent (Fig. 4B–F). After heat shocks at 4.7 hpf, *zic1* expression is observed extending to the anterior tip of these embryos (Fig. 4C, arrowhead). The absence of *otx2b* (diencephalon and midbrain, Fig. 4C') and anterior shift of *egr2b* (hindbrain rhombomeres 3 and 5, Fig. 4C") suggests that the observed *zic1* expression reflects its hindbrain expression domain. Heat shock at 6 hpf produces a similar result, though *egr2b* expression is not shifted as far anteriorly (Fig. 4D–D"). In contrast, heat shocking at 8 hpf does not suppress *otx2b* (Fig. 4E') and *egr2b* expression is shifted only mildly anteriorly (Fig. 4E"), suggesting that the *zic1* expression observed may correspond to either diencephalic or midbrain identity. Heat shocks at 9 hpf produce a similar result (Fig. 4F–F"). These experiments suggest that forebrain expression can be suppressed by Wnt signaling throughout gastrulation, while midbrain fate becomes resistant to Wnt suppression between 6 and 8 hpf. The binary responses of forebrain and midbrain contrast with the graded anterior shift in hindbrain fate with timed Wnt overexpression.

To determine how rapidly *otx2b* regulation responds to Wnt overexpression, we repeated our *hs:wnt8a*/+ activation at the same time points but analyzed gene expression at 10 hpf (Fig. 5). After heat shocking at either 4.7 or 6 hpf, *otx2b* is completely suppressed in the neural plate at 10 hpf (Fig. 5B,D; some prechordal mesodermal cells that transiently express *otx2b* at this stage retain some *otx2b*, see Fig. 6L). In contrast, *otx2b* is not affected after heat shocks at 8 or 9 hpf (Fig. 5F,H). The resistance of neural plate *otx2b* to Wnt-mediated suppression at 8 hpf is not simply a matter of the short period between heat shock and subsequent analysis, as *otx2b* is normal when analyzed 4 h later (Figs. S4A and B).

The binary response of *otx2b* to Wnt overexpression was unexpected, since Wnt signaling during this developmental period is thought to regulate neural plate polarization in a graded fashion, which would predict a variable response by *otx2b*. We therefore assayed the

additional neural plate patterning markers *otx1, gbx1*, and *her5* at 10 hpf. After heat shocking at 4.7 hpf, *otx1* in the anterior neural plate is also suppressed at 10 hpf, while *gbx1* is expanded into the anterior neural plate but with a large medial gap in staining, and *her5* appears as a disorganized medial domain (Fig. 5J,R,Z). After heat shocking at 6 hpf, *otx1* is slightly reduced, while *gbx1* appears roughly normally positioned, but with low level ectopic staining in the posterior neural plate, and *her5* is slightly disorganized with scattered expressing cells anterior to the normal domain (Fig. 5L,T,B'). After heat shocking at either 8 or 9 hpf, *otx1, gbx1*, and *her5* appear roughly normal at 10 hpf (Fig. 5N,V,D',P,X,F').

These results demonstrate that the mechanisms responsible for early regulation of *otx2b* and *gbx1* operate independently, as *otx2b* repression is observed in the absence of *gbx1* anterior expansion after heat shocks at 6 hpf (cf. Fig. 5D,T). By 6 h after administration of the heat shock at 6 hpf (i.e. at 12 hpf), *gbx1* expansion into the anterior neural plate is observed, correlating with absence of both *otx1* and *otx2b* (Figs. S4C–F and Fig. 5D). Thus, while our data support independent modes of early regulation, they are also consistent with the known antagonistic relationship between *otx* and *gbx* genes (Joyner et al., 2000; Li and Joyner, 2001; Millet et al., 1999; Simeone, 2000; Wassarman et al., 1997).

### 3.4. otx2b is directly repressed by Wnt signaling

The above results suggest a close relationship between Wnt signaling and *otx2b* regulation that mechanistically changes between 6-8 hpf, but an alternate possibility is that neural plate cells change in their ability to respond to the ectopic Wnt ligand expressed from the transgene. To test this, we induced Wnt signaling intracellularly with BIO, a small molecule Gsk3-β inhibitor (Sato et al., 2004). Treatment of embryos with 10 μM BIO at 6, 8, and 9 hpf caused loss of eyes at 27 hpf, mimicking the effects of *hs:wnt8a* at these time points (Fig. 6B,C,D). In addition, treatment with BIO at 6 hpf suppressed midbrain development as indicated by loss of *dmbx1a* and *otx2b* expression (Fig. 6B) and produced a concomitant anterior shift of *egr2b* (Fig. 6F), phenocopying the effects of *hs:wnt8a*. Importantly, BIO treatment at 8 hpf did not suppress midbrain fate (Fig. 6C) and treated embryos showed a correspondingly milder anterior shift of *egr2b* (Fig. 6G), effects that are also observed, though milder, after BIO treatment at 9 hpf (Fig. 6D,H). Thus, BIO treatment recapitulates all key aspects of *hs:wnt8a* treatments, supporting the argument that the change in *otx2b* regulation by Wnt reflects a property of the *otx2b* locus rather than a change in the cellular reception of ectopic Wnt ligand.

We next tested whether Wnt-mediated *otx2b* repression is direct or requires a protein intermediate by combining BIO treatment with the translation inhibitor cycloheximide (CHX). As a control, embryos treated with CHX at 6 or 8 hpf did not show a change in the expression pattern of *otx2b* at 10 hpf, and *gbx1* was only mildly affected (Fig. 6I–K; N–P), and treatment with BIO alone at 6 hpf, but not 8 hpf, suppressed *otx2b* in the neural plate (insets in Fig. 6L,M). In contrast, BIO treatment at 6 hpf was able to repress neural plate *otx2b* expression in the presence of CHX (Fig. 6L) but treatment at 8 hpf could not (Fig. 6M), indicating that *otx2b* repression after the 6 hpf treatment occurs in the absence of new protein synthesis. *gbx1* expression was not expanded anteriorly after treatment at either time point (Fig. 6Q,R), thereby confirming that changes in anteroposterior patterning per se were

not responsible for *otx2b* regulation. Thus, our results argue that *otx2b* is directly repressed in the neural plate by Wnt signaling at its onset, but a transition occurs by 8 hpf such that *otx2b* is no longer Wnt responsive.

### 3.5.   Timed Wnt modulation induces a rapid and dynamic transcriptional response

Our results argue that phase one comprises a period of dynamic transcriptional responses to Wnt signaling in the neural plate. To test this further, we performed four RNA-Seq analyses after activation or inhibition of Wnt signaling during sub-portions of phase one (experimental design shown in Fig. S5). Briefly, *hs:dkk1b*/+ and *hs:wnt8a*/+ embryos were first heat shocked from 5-6 hpf or 5.5–6 hpf, respectively, then collected at 7 hpf for analysis ("5→7 hpf"), or heat shocked from 7-8 or 7.5-8 hpf, respectively, and collected at 9 hpf ("7→9 hpf"). RNA was extracted from transgenic embryos or their wild-type siblings, then subjected to RNA-seq differential gene expression analysis (see Materials and Methods). Genes with fold change    2 and FDR    .05 were considered significantly changed.

Overall, under each of our experimental conditions, only a relatively small number of genes showed significantly changed expression, with down-regulated genes outnumbering upregulated genes approximately 3:1 (Fig. 7, Supplemental Tables 1–4) with implications regarding Wnt impact on neural AP patterning. In the 5→7 hpf experiment, Wnt suppression and Wnt activation result in gene expression changes suggestive of maintenance of posterior neural gene expression; i.e. Wnt suppression (*hs:dkk1b*) reduces posterior neural genes (*gbx1, znf503, znf703, znfl1h*), but does not increase anterior neural genes, while Wnt activation (*hs:wnt8a*) suppresses anterior neural plate markers (*otx1, otx2b, otx2a, shisa2a*), but posterior neural markers are not significantly altered (Supplemental Tables 1 and 2; Fig. 7A,B). In the 7→9 hpf experiment, the same trends continue (Fig. 7C,D), but with an increased number of identified differentially expressed genes. Thus, Wnt inhibition (*hs:dkk1b*) results in suppression of posterior neural gene expression (18 genes), but not elevation of anterior neural gene expression (2 exceptions), and Wnt activation (*hs:wnt8a*) suppresses anterior neural gene expression (17 genes), but does not alter posterior neural gene expression (Fig. 7C,D, Supplemental Tables 3 and 4). Together, this suggests Wnt signaling is required, but not sufficient, for posterior neural plate gene expression, and Wnt signaling is strongly antagonistic to anterior neural plate identity.

Our data also reveal dynamic aspects of the cellular response to Wnt signaling. While 17/18 genes that require Wnt signaling at 5–7 hpf (downregulated *in hs:dkk1b*) continue to be dependent on Wnt signaling at 7–9 hpf (Supp. Tables 1,2), only 7/18 genes responsive to *hs:wnt8a* at 5–7 hpf continue to be responsive at 7–9 hpf (Supp. Tables 3,4).

The dynamism of the transcriptional response to Wnt is exemplified by Wnt pathway genes. For instance, *dkk1b* is induced by activated Wnt at both timepoints, and though our experimental design does not allow us to determine Wnt necessity for *dkk1b* expression, this relationship has experimental support (Hino et al., 2018; Nusse and Clevers, 2017). In contrast, while Wnt signaling is both necessary and sufficient for *axin2* expression at 5–7 hpf, Wnt is necessary but not sufficient for *axin2* at 7–9 hpf (Supp. Tables 1–4). This result may reflect the rapid induction and decline of *axin2* levels (Fig. S1). *nkd1* and *tpbga*, which both encode Wnt pathway negative regulatory proteins (Malinauskas and Jones, 2014;

Schneider et al., 2010) require Wnt signaling at both time points, but Wnt activation is sufficient to induce their elevated expression only at 7–9 hpf. Other genes also show a dichotomous relationship to Wnt signaling in our datasets. Consistent with Figs. 4–6, *otx2b* is downregulated at 5–7 hpf, but not at 7–9 hpf by *hs:wnt8a*. Additionally, two genes expressed in prechordal plate change responses to ectopic Wnt: whereas *he1.1* is induced by *hs:wnt8a* at 5–7 hpf, it is suppressed at 7–9 hpf, and *tent5ba* was activated by *hs:wnt8a* at 5–7 hpf, but was unaffected at 7–9 hpf. Thus, the transcriptional response of Wnt regulated genes is dynamic and heterogeneous, with fundamentally different responses being observed before and after 7 hpf.

We detected nine genes for which Wnt signaling is both necessary and sufficient in our datasets, with none in common to 5–7 and 7–9 hpf. At 5–7 hpf, *axin2* is the only representative of this class of gene targets. At 7–9 hpf, we identified the Wnt pathway genes *nkd1* and *tpbga, pax3a* (expressed in the neural plate border), *prrx1b*, one unknown gene, and three genes expressed in the midbrain-hindbrain boundary, *wnt8b, en2a* and *her5*. That these three MHB genes have clear relationships to Wnt signaling (Buckles et al., 2004; Danielian and McMahon, 1996; Kim et al., 2002; Lekven et al., 2003; McGrew et al., 1999) raises the possibility that they interact in a feedback loop established downstream of primary AP patterning Wnt signaling (see discussion).

### 3.6. Changes in level of transcription of AP patterning genes do not correspond to changes in domain size

To validate the RNA-Seq findings and to observe the relationship between changes in transcription and AP neural plate patterning, we performed in situ hybridizations against a selection of genes that were affected in at least one of the treatment conditions. In *hs:dkk1b*/+ embryos, *tpbga* staining in the margin is visibly reduced in both the 5→7 hpf and 7→9 hpf experiments (Fig. 8A,B), matching the 2–3 fold decrease measured by RNA-seq (Supplemental Tables 1 and 2). *lef1* and *her5* appeared identical in control and experimental embryos at 7 hpf, but were visibly reduced in *hs:dkk1b* embryos at 9 hpf (Fig. 8C–F). Though RNA-seq measurements showed *gbx1* downregulation in both 5–7 hpf and 7–9 hpf experiments, it was difficult to see differences by in situ hybridization, perhaps reflecting the difficulty in its detection and low expression levels (Fig. 8G,H). *otx2b* also appeared the same in *hs:dkk1b*/+ and +/+ siblings (Fig. 8I,J). In all cases, Wnt suppression in this experimental paradigm did not appear to change the AP position of any gene expression domains, indicating that transcriptional level changes precede AP patterning changes.

We used the same probes to analyze *hs:wnt8a*/+ embryos in both experiments. While *tpbga* appears unchanged in the 5→7 hpf experiment (Fig. 9A), staining is visibly stronger in the 7→9 hpf experiment, though no change in AP pattern is observed (Fig. 9B). *lef1* staining appears mildly stronger at 7 hpf (Fig. 9C), though the RNA-seq analysis did not measure a significant difference in levels (this could be attributed to low statistical power, see materials and methods). In contrast, staining is equivalent in *hs:wnt8a*/+ and wild-type sibling embryos at 9 hpf (Fig. 9D). *her5* provided the only example of a change in expression pattern: at 7 hpf, *hs:wnt8a* embryos show scattered *her5*^{+} cells, though these appear to be in

the mes/r1 region, and no difference in transcript levels is measured (Fig. 9E). At 9 hpf, *her5* is expanded anteriorly, consistent with the measured 2-fold increase in expression (Fig. 9F). Consistent with results shown in Fig. 5, *gbx1* appears unaltered at either time point (Fig. 9G,H), and *otx2b* is reduced in intensity at 7 hpf, but is not visibly different at 9 hpf (Fig. 9I,J). Therefore, with the exception of *her5*, the most rapid response to Wnt pathway activation during gastrulation is a change to the transcription levels of a small number of genes without a change in the AP fates of the expressing cells.

## 4.    Discussion

### 4.1.    Wnt-mediated neural patterning is divided into distinct temporal phases

We have used temporal control of Wnt signaling to show that it influences global neural plate patterning in zebrafish in three distinct phases (Fig. 10). The first phase, which we define as the primary AP patterning phase, occurs during gastrulation (between 4-9.5 hpf). During this time period, Wnt signaling, likely stimulated by *wnt8a*, acts across the neural plate to establish the progenitor cell allocations to gross brain divisions. This function is mediated through two types of rapid transcriptional responses: repression of anterior neural genes, including direct repression of *otx2b*, and indirect activation of hindbrain genes. The second phase, which we refer to as the mes/r1 phase, occurs during early neurulation (between 9.5 and 12 hpf). In response to primary AP patterning, Wnt ligands, i.e. *wnt8b* and *wnt1*, are expressed in the mes/r1 domain of the neural plate, and reinforce mes/r1 identity, likely through regulation of *en2a*, which prevents expansion of forebrain gene expression into midbrain territory. *Otx2b* expression is resistant to Wnt-mediated repression at this stage, thus the *otx2/gbx* interface can be maintained in the presence of active Wnt signaling. Signaling during this period also feeds into the MHB gene regulatory network (GRN) to maintain MHB fate. Finally, during segmentation (between 12 and 17 hpf), Wnt signaling maintains the MHB GRN to enable proper MHB morphogenesis.

### 4.2.    The neural plate transcriptional response to Wnt signaling is dynamic

Our findings show that the response of the neural plate to Wnt signaling changes as the embryo develops, and that transcriptional responses to Wnt stimulation are dynamic. For example, intracellular Wnt transduction activates Wnt pathway genes in distinct ways: e.g., while *axin2* is induced rapidly and decays rapidly, *dkk1b* is induced rapidly and decays more slowly (thus enabling its detection in both timed experiments). Additionally, the antagonists *nkd2* and *tpbga* are only induced by ectopic Wnt under undetermined circumstances of cellular compentency (i.e. only at 7–9 hpf). In support of this, *tpbga* is induced by ectopic Wnt, but only in the normal expression pattern with greater transcript abundance (Fig. 9B). Indeed, our in situ hybridization analyses show that, of genes that are differentially regulated by Wnt, all but one show immediate changes in transcript abundance without changes in their spatial pattern of expression. Thus, we suggest that the immediate response to Wnt signaling in the neural plate is the normal establishment of gene expression levels rather than their spatial pattern per se.

One function of Wnt signaling during neural patterning is to regulate Tcf proteins. Prior studies of *tcf7l1* orthologs in neural patterning suggested that Wnt-mediated brain patterning

could be modeled as graded de-repression of *tcf7l1*-repressed gene targets (Dorsky et al., 2003; Kim et al., 2000). Zebrafish embryos lacking *tcf7l* function show rostral expansion of midbrain and MHB genes concomitant with loss of forebrain, a phenotype that is rescued by *wnt8a* loss of function (Dorsky et al., 2003) . Our data suggest that the presence of Tcf7l proteins prevents the precocious suppression of anterior neural plate genes, and thus the expansion of MHB gene expression observed in *tcf7l* mutants (Chitnis and Itoh, 2004; Dorsky et al., 2003; Kim et al., 2000). While our data do not rule out the graded de-repression model, they also suggest that the process may be complex, as we show that at least one gene, *otx2b*, is a target of direct Wnt-repression. Several Wnt-repression targets are known, and repression may potentially involve steric interference of activator binding (Piepenburg et al., 2000), binding of activated β-catenin-Tcf or β-catenin-Lefi complexes with a co-repressor (Jamora et al., 2003; Theisen et al., 2007), or involvement of an alternative Tcf "helper" binding site that engages the C-clamp domain found in some Tcf proteins (Zhang et al., 2014). Identifying the mechanism of target gene regulation will be an important step in understanding the patterning mechanism.

An intriguing aspect of *otx2b* regulation by Wnt signaling is the conversion of the *otx2b* locus from responsive to non-responsive around the 7 hpf time point. *otx2b* is not alone in this response switch, e.g. *hel.1* is activated by Wnt at 5–7 hpf and repressed at 7–9 hpf. Another switch occurs at this same time point: biphasic *wnt8a* transcription in the embryonic margin switches from Nodal to Brachyury-dependent regulation of a margin enhancer (Narayanan and Lekven, 2012; Narayanan et al., 2011). Determining whether these transitions are mechanistically linked will require further study.

### 4.3.   Wnt signaling sets boundaries to establish brain domains

Our findings provide a model framework to reconcile the known diverse roles of Wnt signaling in regulation of neural AP patterning. It has recently been shown that the initial regionalization that partitions the spinal cord from the rest of the nervous system occurs prior to neural induction (Metzis et al., 2018). Our results provide further evidence that the next step of nervous system regionalization involves the establishment of compartment interfaces separating first midbrain and hindbrain followed by forebrain and midbrain. Wnt8a positions the midbrain-hindbrain boundary (MHB) through its suppression of *otx2b* and facilitation of *gbx1* activation (Rhinn et al., 2005, 2009). However, at 7 hpf, *otx2b* becomes refractory to Wnt-mediated suppression. This causes the position of the MHB to become fixed along the AP axis, as *gbx1* cannot expand anteriorly into *otx2*^{+} cells. The secondary patterning phase can be seen as the fixing of another major interface, the diencephalic-mesencephalic boundary (DMB) (Scholpp and Brand, 2003) as well as refinement within the mes/r1 region. In this case, our results suggest an autoregulatory mes/r1 feedback module comprising *wnt8b*, *en2a*, and *her5* activated downstream of primary phase Wnt8a signaling, as Wnt signaling is both necessary and sufficient for their regulation. mes/r1 Wnt signaling maintains midbrain identity, but *wnt8b* also controls diencephalon patterning (Houart et al., 2002; Kim et al., 2002). Because locking the MHB and DMB in position on the AP axis ultimately determines the size of the relative regions of the brain, these findings show that the regionalization of the neural ectoderm occurs in a temporally progressive manner starting at the most posterior end prior to neural induction and

progressing anteriorly. Through this step-wise mechanism, Wnt-mediated patterning occurs in a series of temporally distinct events that must occur in the correct order to properly pattern the neural plate AP axis.

### 4.4    Integrating models of Wnt transport and neural AP patterning

Considerable evidence supports the model that Wnt signaling functions in a dose-dependent manner to pattern the neural plate AP axis, and several models have been proposed for how these doses could be generated (Chitnis and Itoh, 2004; Elkouby and Frank, 2010; Niehrs, 2004). This has classically been explained with a model where Wnt8a, secreted from its posterior paraxial mesoderm source, diffuses anteriorly to form a concentration gradient (Kiecker and Niehrs, 2001). This model has been challenged recently with the discovery of filopodial delivery of Wnt8a from cells in the zebrafish embryonic margin (Mattes et al., 2018; Stanganello et al., 2015). While the filopodial transport model resolves the conundrum of diffusion of hydrophobic Wnt ligands, one potential issue is that filopodial delivery of Wnt8a would be predicted to have a signaling range restricted to the length of filopodia, i.e. closer to the margin, than would be possible through diffusion (Green et al., 2015), though modeling studies of Wnt8a-induced filopodial dynamics suggests this mode of delivery can affect cells at considerable distances, given enough time (Mattes et al., 2018). Our results provide a potential framework in support of the filopodial delivery model: during the early epiboly stages that Wnt8a-mediated patterning occurs, most neural plate progenitor cells are within several cell diameters of Wnt8a-expressing marginal cells. The mes/r1 phase of patterning then initiates by 9.5 hpf, when the embryonic margin has migrated vegetally and would potentially be beyond the range in which filopodia containing Wnt8a can influence patterning further.

## 5.    Conclusion

We have investigated the temporal elements of Wnt-mediated neural patterning and have provided evidence that Wnt-mediated neural patterning can be divided into three distinct temporal phases. These phases are established both by the Wnt ligands involved, including Wnt8a and mes/r1 expressed ligands, and differential transcriptional responses of neural plate progenitor cells to Wnt signaling itself. The mechanics of neural posterization also occurs in a predictable time line, with the suppression of anterior neural fate occurring prior to posterior gene expansion. Finally, we establish that the response of different Wnt receptive genes to Wnt signaling takes different periods of time in a manner that is independent of the directness of the response. These findings broaden our understanding of the mechanisms that drive Wnt-mediated neural patterning and may serve an important function in understanding the causes of patterning defects underlying a wide range of neuropathologies in humans.

## Supplementary Material

Refer to Web version on PubMed Central for supplementary material.

## Acknowledgements

## References

Ahn VE, Chu ML, Choi HJ, Tran D, Abo A, Weis WI, 2011 Structural basis of Wnt signaling inhibition by Dickkopf binding to LRP5/6. Dev. Cell 21, 862–873. [PubMed: 22000856]

Baker KD, Ramel MC, Lekven AC, 2010 A direct role for Wnt8 in ventrolateral mesoderm patterning. Dev. Dynam 239, 2828–2836.

Buckles GR, Thorpe CJ, Ramel MC, Lekven AC, 2004 Combinatorial Wnt control of zebrafish midbrain-hindbrain boundary formation. Mech. Dev 121, 437–447. [PubMed: 15147762]

Chitnis AB, Itoh M, 2004 Exploring alternative models of rostral-caudal patterning in the zebrafish neurectoderm with computer simulations. Curr. Opin. Genet. Dev 14, 415–421. [PubMed: 15261658]

Cox WG, Hemmati-Brivanlou A, 1995 Caudalization of neural fate by tissue recombination and bFGF. Development 121, 4349–4358. [PubMed: 8575335]

Danielian PS, McMahon AP, 1996 Engrailed-1 as a target of the Wnt-1 signalling pathway in vertebrate midbrain development. Nature 383, 332–334. [PubMed: 8848044]

Dorsky RI, Itoh M, Moon RT, Chitnis A, 2003 Two tcf3 genes cooperate to pattern the zebrafish brain. Development 130, 1937–1947. [PubMed: 12642497]

Durston AJ, Timmermans JP, Hage WJ, Hendriks HF, de Vries NJ, Heideveld M, Nieuwkoop PD, 1989 Retinoic acid causes an anteroposterior transformation in the developing central nervous system. Nature 340, 140–144. [PubMed: 2739735]

Edgar R, Domrachev M, Lash AE, 2002 Gene Expression Omnibus: NCBI gene expression and hybridization array data repository. Nucleic Acids Res. 30, 207–210. [PubMed: 11752295]

Elkouby YM, Frank D, 2010 Wnt/beta-Catenin Signalling in Vertebrate Posterior Neural Development, 2011/04/01 Ed. Morgan & Claypool Life Sciences, San Rafael (CA).

Erter CE, Wilm TP, Basler N, Wright CV, Solnica-Krezel L, 2001 Wnt8 is required in lateral mesendodermal precursors for neural posteriorization in vivo. Development 128, 3571–3583. [PubMed: 11566861]

Farrell JA, Wang Y, Riesenfeld SJ, Shekhar K, Regev A, Schier AF, 2018 Singlecell reconstruction of developmental trajectories during zebrafish embryogenesis. Science 360.

Gibbs HC, Chang-Gonzalez A, Hwang W, Yeh AT, Lekven AC, 2017 Midbrain-hindbrain Boundary morphogenesis: at the intersection of wnt and fgf signaling. Front. Neuroanat 11, 64. [PubMed: 28824384]

Green D, Whitener AE, Mohanty S, Lekven AC, 2015 Vertebrate nervous system posteriorization: grading the function of Wnt signaling. Dev. Dynam 244, 507–512.

Hino H, Nakanishi A, Seki R, Aoki T, Yamaha E, Kawahara A, Shimizu T, Hibi M, 2018 Roles of maternal wnt8a transcripts in axis formation in zebrafish. Dev. Biol 434, 96–107. [PubMed: 29208373]

Houart C, Caneparo L, Heisenberg C, Barth K, Take-Uchi M, Wilson S, 2002 Establishment of the telencephalon during gastrulation by local antagonism of Wnt signaling. Neuron 35, 255–265. [PubMed: 12160744]

Hsieh JC, Rattner A, Smallwood PM, Nathans J, 1999 Biochemical characterization of Wnt-frizzled interactions using a soluble, biologically active vertebrate Wnt protein. Proc. Natl. Acad. Sci. U. S. A 96, 3546–3551. [PubMed: 10097073]

Jamora C, DasGupta R, Kocieniewski P, Fuchs E, 2003 Links between signal transduction, transcription and adhesion in epithelial bud development. Nature 422, 317–322. [PubMed: 12646922]

Jho EH, Zhang T, Domon C, Joo CK, Freund JN, Costantini F, 2002 Wnt/beta-catenin/Tcf signaling induces the transcription of Axin2, a negative regulator of the signaling pathway. Mol. Cell Biol 22, 1172–1183. [PubMed: 11809808]

Joyner AL, Liu A, Millet S, 2000 Otx2, Gbx2 and Fgf8 interact to position and maintain a mid-hindbrain organizer. Curr. Opin. Cell Biol 12, 736–741. [PubMed: 11063941]

Kelly GM, Greenstein P, Erezyilmaz DF, Moon RT, 1995 Zebrafish wnt8 and wnt8b share a common activity but are involved in distinct developmental pathways. Development 121, 1787–1799. [PubMed: 7600994]

Kiecker C, Niehrs C, 2001 A morphogen gradient of Wnt/beta-catenin signalling regulates anteroposterior neural patterning in Xenopus. Development 128, 4189–4201. [PubMed: 11684656]

Kim CH, Oda T, Itoh M, Jiang D, Artinger KB, Chandrasekharappa SC, Driever W, Chitnis AB, 2000 Repressor activity of Headless/Tcf3 is essential for vertebrate head formation. Nature 407, 913–916. [PubMed: 11057671]

Kim SH, Shin J, Park HC, Yeo SY, Hong SK, Han S, Rhee M, Kim CH, Chitnis AB, Huh TL, 2002 Specification of an anterior neuroectoderm patterning by Frizzled8a-mediated Wnt8b signalling during late gastrulation in zebrafish. Development 129, 4443–4455. [PubMed: 12223403]

Kishimoto Y, Lee KH, Zon L, Hammerschmidt M, Schulte-Merker S, 1997 The molecular nature of zebrafish swirl: BMP2 function is essential during early dorsoventral patterning. Development 124, 4457–4466. [PubMed: 9409664]

Kudoh T, Wilson SW, Dawid IB, 2002 Distinct roles for Fgf, Wnt and retinoic acid in posteriorizing the neural ectoderm. Development 129, 4335–4346. [PubMed: 12183385]

Langenberg T, Brand M, 2005 Lineage restriction maintains a stable organizer cell population at the zebrafish midbrain-hindbrain boundary. Development 132, 3209–3216. [PubMed: 15958515]

Lekven AC, Buckles GR, Kostakis N, Moon RT, 2003 Wnt1 and wnt10b function redundantly at the zebrafish midbrain-hindbrain boundary. Dev. Biol 254, 172–187. [PubMed: 12591239]

Lekven AC, Thorpe CJ, Waxman JS, Moon RT, 2001 Zebrafish *wnt8* encodes two Wnt8 proteins on a bicistronic transcript and is required for mesoderm and neurectoderm patterning. Dev. Cell 1, 103–114. [PubMed: 11703928]

Li JY, Joyner AL, 2001 Otx2 and Gbx2 are required for refinement and not induction of mid-hindbrain gene expression. Development 128, 4979–4991. [PubMed: 11748135]

Malinauskas T, Jones EY, 2014 Extracellular modulators of Wnt signalling. Curr. Opin. Struct. Biol 29, 77–84. [PubMed: 25460271]

Matsuo I, Kuratani S, Kimura C, Takeda N, Aizawa S, 1995 Mouse Otx2 functions in the formation and patterning of rostral head. Genes Dev. 9, 2646–2658. [PubMed: 7590242]

Mattes B, Dang Y, Greicius G, Kaufmann LT, Prunsche B, Rosenbauer J, Stegmaier J, Mikut R, Ozbek S, Nienhaus GU, Schug A, Virshup DM, Scholpp S, 2018 Wnt/PCP controls spreading of Wnt/beta-catenin signals by cytonemes in vertebrates. Elife 7.

McGrew LL, Hoppler S, Moon RT, 1997 Wnt and FGF pathways cooperatively pattern anteroposterior neural ectoderm in Xenopus. Mech. Dev 69, 105–114. [PubMed: 9486534]

McGrew LL, Lai CJ, Moon RT, 1995 Specification of the anteroposterior neural axis through synergistic interaction of the Wnt signaling cascade with noggin and follistatin. Dev. Biol 172, 337–342. [PubMed: 7589812]

McGrew LL, Takemaru K, Bates R, Moon RT, 1999 Direct regulation of the Xenopus engrailed-2 promoter by the Wnt signaling pathway, and a molecular screen for Wnt-responsive genes, confirm a role for Wnt signaling during neural patterning in Xenopus. Mech. Dev 87, 21–32. [PubMed: 10495268]

McMahon AP, Bradley A, 1990 The Wnt-1 (int-1) proto-oncogene is required for development of a large region of the mouse brain. Cell 62, 1073–1085. [PubMed: 2205396]

Metzis V, Steinhauser S, Pakanavicius E, Gouti M, Stamataki D, Ivanovitch K, Watson T, Rayon T, Mousavy Gharavy SN, Lovell-Badge R, Luscombe NM, Briscoe J, 2018 Nervous system

Author Manuscript

Author Manuscript

Author Manuscript

Author Manuscript

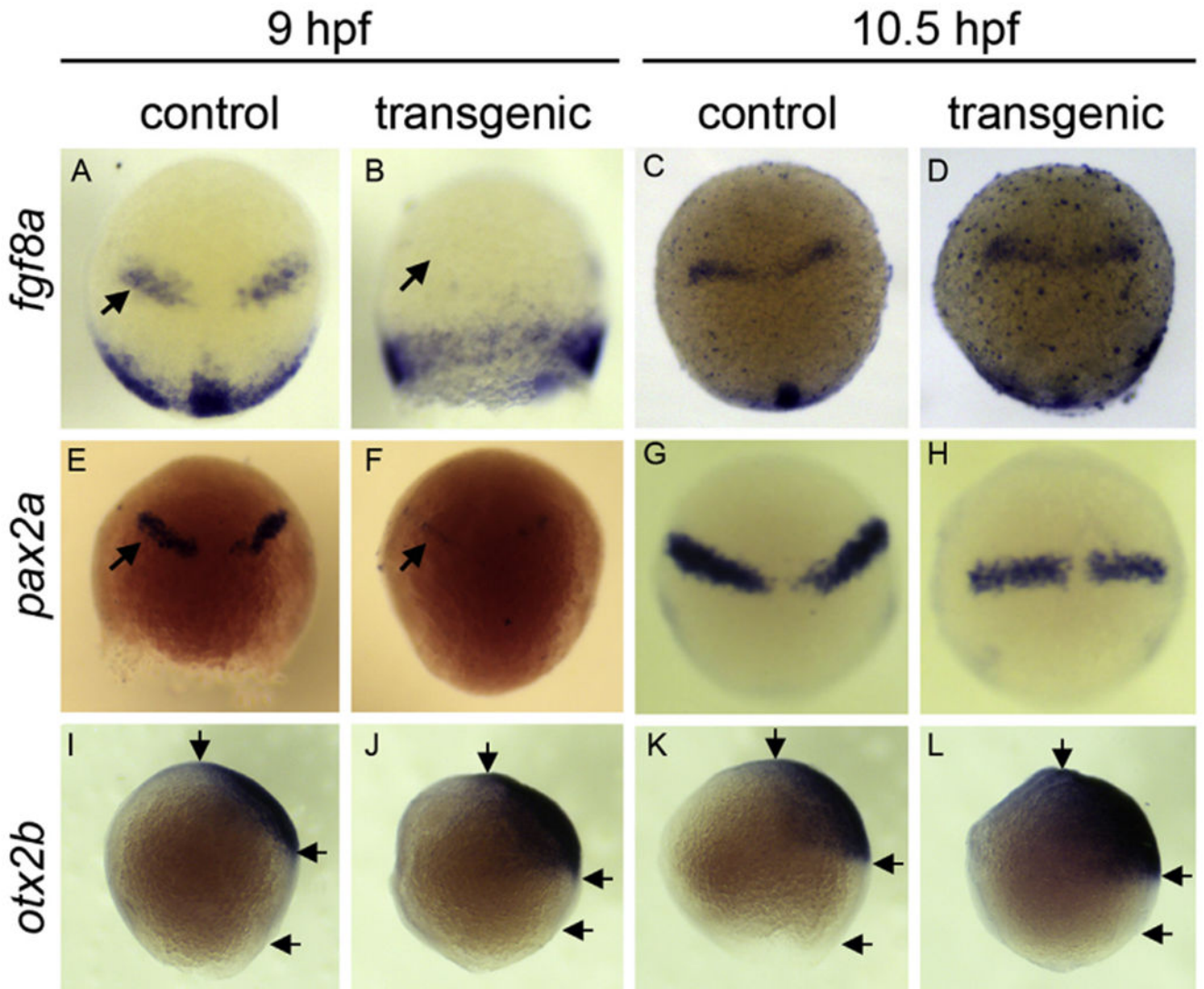regionalization entails axial allocation before neural differentiation. Cell 175, 1105–1118 e1117. [PubMed: 30343898]

Millet S, Campbell K, Epstein DJ, Losos K, Harris E, Joyner AL, 1999 A role for Gbx2 in repression of Otx2 and positioning the mid/hindbrain organizer. Nature 401, 161–164. [PubMed: 10490024]

Momoi A, Yoda H, Steinbeisser H, Fagotto F, Kondoh H, Kudo A, Driever W, Furutani-Seiki M, 2003 Analysis of Wnt8 for neural posteriorizing factor by identifying Frizzled 8c and Frizzled 9 as functional receptors for Wnt8. Mech. Dev 120, 477–489. [PubMed: 12676325]

Narayanan A, Lekven AC, 2012 Biphasic wnt8a expression is achieved through interactions of multiple regulatory inputs. Dev. Dynam 241, 1062–1075.

Narayanan A, Thompson SA, Lee JJ, Lekven AC, 2011 A transgenic *wnt8a:PAC* reporter reveals biphasic regulation of vertebrate mesoderm development. Dev. Dynam 240, 898–907.

Niehrs C, 2004 Regionally specific induction by the Spemann-Mangold organizer. Nat. Rev. Genet 5, 425–434. [PubMed: 15153995]

Nieuwkoop PD, 1952 Activation and organisation of the central nervous system in amphibians. J. Exp. Zool 120, 1–108.

Nordstrom U, Jessell TM, Edlund T, 2002 Progressive induction of caudal neural character by graded Wnt signaling. Nat. Neurosci 5, 525–532. [PubMed: 12006981]

Nusse R, Clevers H, 2017 Wnt/beta-Catenin signaling, disease, and emerging therapeutic modalities. Cell 169, 985–999. [PubMed: 28575679]

Piepenburg O, Vorbruggen G, Jackle H, 2000 Drosophila segmentborders result from unilateral repression of hedgehog activity by wingless signaling. Mol. Cell 6, 203–209. [PubMed: 10949042]

Polevoy H, Gutkovich YE, Michaelov A, Volovik Y, Elkouby YM, Frank D, 2019 New roles for Wnt and BMP signaling in neural anteroposterior patterning. EMBO Rep. 20.

Raj B, Wagner DE, McKenna A, Pandey S, Klein AM, Shendure J, Gagnon JA, Schier AF, 2018 Simultaneous single-cell profiling of lineages and cell types in the vertebrate brain. Nat. Biotechnol 36, 442–450. [PubMed: 29608178]

Ramel MC, Buckles GR, Lekven AC, 2004 Conservation of structure and functional divergence of duplicated Wnt8s in pufferfish. Dev. Dynam 231, 441–448.

Rhinn M, Lun K, Ahrendt R, Geffarth M, Brand M, 2009 Zebrafish gbx1 refines the midbrain-hindbrain boundary border and mediates the Wnt8 posteriorization signal. Neural Dev. 4, 12. [PubMed: 19341460]

Rhinn M, Lun K, Luz M, Werner M, Brand M, 2005 Positioning of the midbrain-hindbrain boundary organizer through global posteriorization of the neuroectoderm mediated by Wnt8 signaling. Development 132, 1261–1272. [PubMed: 15703279]

Robinson MD, Oshlack A, 2010 A scaling normalization method for differential expression analysis of RNA-seq data. Genome Biol. 11, R25. [PubMed: 20196867]

Sato N, Meijer L, Skaltsounis L, Greengard P, Brivanlou AH, 2004 Maintenance of pluripotency in human and mouse embryonic stem cells through activation of Wnt signaling by a pharmacological GSK-3-specific inhibitor. Nat. Med 10, 55–63. [PubMed: 14702635]

Schneider I, Schneider PN, Derry SW, Lin S, Barton LJ, Westfall T, Slusarski DC, 2010 Zebrafish Nkd1 promotes Dvl degradation and is required for left-right patterning. Dev. Biol 348, 22–33. [PubMed: 20858476]

Scholpp S, Brand M, 2003 Integrity of the midbrain region is required to maintain the diencephalic-mesencephalic boundary in zebrafish no isthmus/pax2.1 mutants. Dev. Dynam 228, 313–322.

Simeone A, 2000 Positioning the isthmic organizer where Otx2 and Gbx2meet. Trends Genet. 16, 237–240. [PubMed: 10827447]

Stanganello E, Hagemann AI, Mattes B, Sinner C, Meyen D, Weber S, Schug A, Raz E, Scholpp S, 2015 Filopodia-based Wnt transport during vertebrate tissue patterning. Nat. Commun 6, 5846. [PubMed: 25556612]

Stoick-Cooper CL, Weidinger G, Riehle KJ, Hubbert C, Major MB, Fausto N, Moon RT, 2007 Distinct Wnt signaling pathways have opposing roles in appendage regeneration. Development 134, 479–489. [PubMed: 17185322]

Theisen H, Syed A, Nguyen BT, Lukacsovich T, Purcell J, Srivastava GP, Iron D, Gaudenz K, Nie Q, Wan FY, Waterman ML, Marsh JL, 2007 Wingless directly represses DPP morphogen expression via an armadillo/TCF/Brinker complex. PloS One 2, e142. [PubMed: 17206277]

Thomas KR, Capecchi MR, 1990 Targeted disruption of the murine int-1 proto-oncogene resulting in severe abnormalities in midbrain and cerebellar development. Nature 346, 847–850. [PubMed: 2202907]

Wassarman KM, Lewandoski M, Campbell K, Joyner AL, Rubenstein JL, Martinez S, Martin GR, 1997 Specification of the anterior hindbrain and establishment of a normal mid/hindbrain organizer is dependent on Gbx2 gene function. Development 124, 2923–2934. [PubMed: 9247335]

Weidinger G, Thorpe CJ, Wuennenberg-Stapleton K, Ngai J, Moon RT, 2005 The Sp1-related transcription factors sp5 and sp5-like act downstream of Wnt/beta-catenin signaling in mesoderm and neuroectoderm patterning. Curr. Biol 15, 489–500. [PubMed: 15797017]

Westerfield M, 2000 The Zebrafish Book. A Guide for the Laboratory Use of Zebrafish (Danio rerio), fourth ed. University of Oregon Press, Eugene.

Wylie AD, Fleming JA, Whitener AE, Lekven AC, 2014 Post-transcriptional regulation of wnt8a is essential to zebrafish axis development. Dev. Biol 386, 53–63. [PubMed: 24333179]

Zervas M, Millet S, Ahn S, Joyner AL, 2004 Cell behaviors and genetic lineages of the mesencephalon and rhombomere 1. Neuron 43, 345–357. [PubMed: 15294143]

Zhang CU, Blauwkamp TA, Burby PE, Cadigan KM, 2014 Wnt-mediated repression via bipartite DNA recognition by TCF in the Drosophila hematopoietic system. PLoS Genet. 10, e1004509. [PubMed: 25144371]
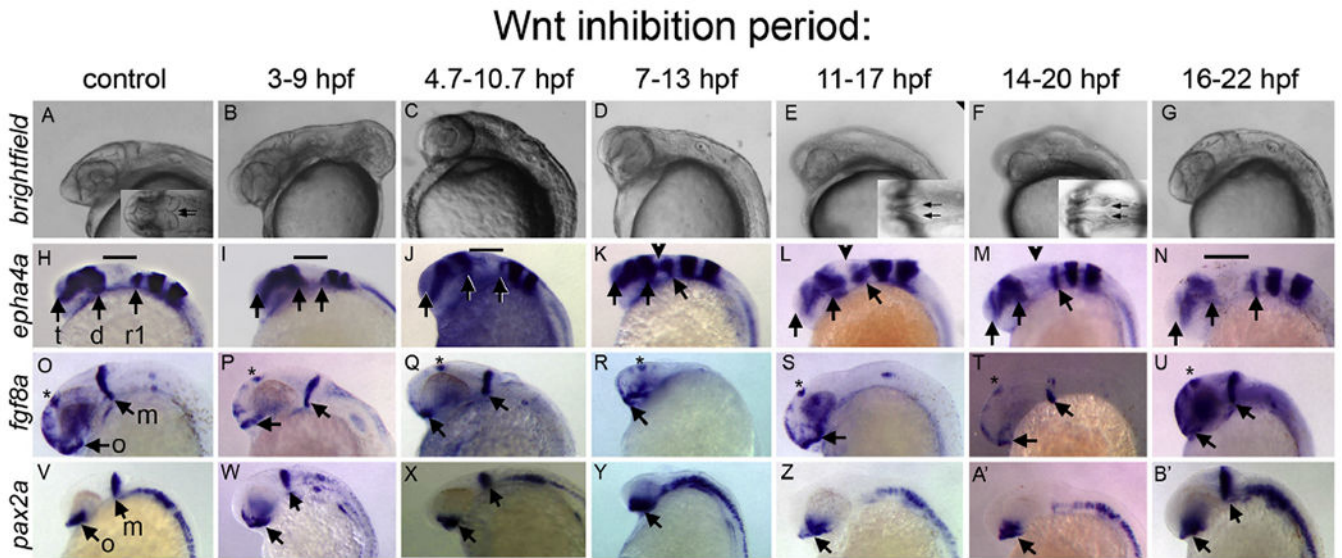
**Fig. 1. Timed inhibition of Wnt/β-catenin signaling reveals distinct neural plate responses.**
Embryos derived from *hs:dkk1b*/+ outcrosses were heat shocked to inhibit Wnt signaling
during the time periods indicated above each column and in Fig. S2. All images: heads of 27
hpf embryos, anterior left, dorsal up. Brightfield (A–G). Insets in (A,E,F) are dorsal views,
arrows indicate inner edge of MHB constrictions, which touch in control embryos. In situ
hybridizations to *epha4a* (H–N), *fgf8a* (O–U), and *pax2a* (V–B'). Wild-type siblings to
*hs:dkk1b*/+ embryos are shown in control (A,H,O,V). Note that Wnt inhibition between 3-9
hpf produces a range of dorsalized phenotypes; C3 dorsalized embryos are shown in
(B,I,P,W). In situ results are equivalent in all dorsalized classes. (H–N) Arrows indicate
telencephalon (t), diencephalon (d), rhombomere 1 (r1). Bar indicates midbrain, MHB and
cerebellar primordia that do not express *epha4a*, indicated with arrowheads in (K,L,M). (O–
B') Arrows indicate optic stalk (o), and mhb (m, when present). Asterisks in (O–U) indicate
dorsal diencephalon domain.

**Fig. 2. Wnt suppression transiently disrupts MHB establishment during epiboly.**
*In situ* hybridization to *fgf8a* (A–D), *pax2a* (E–H), and *otx2b* (I–L). *hs:dkk1b*/+ or +/+
sibling (control) embryos heat shocked at 4.7 hpf, then analyzed at 9 hpf (A,B,E,F,I,J) or
10.5hpf (C,D,G,H,K,L). (A–H) Dorsal view, animal pole up. (I–L) Lateral view, animal pole
up. Note the absence of MHB associated *fgf8a* and *pax2a* at 9 hpf (B,F, arrows) but return of
expression by 10.5 hpf (D,H). Arrows in (I–L) indicate anterior limit of *otx2b*, posterior
limit of *otx2b*, and posterior edge of embryonic margin. Note shortened distance between
the *otx2b* posterior limit relative to the margin in conditions of Wnt loss of function.

# Wnt loss-of-function
## heat shock initiated at 7 hpf, fixed at:
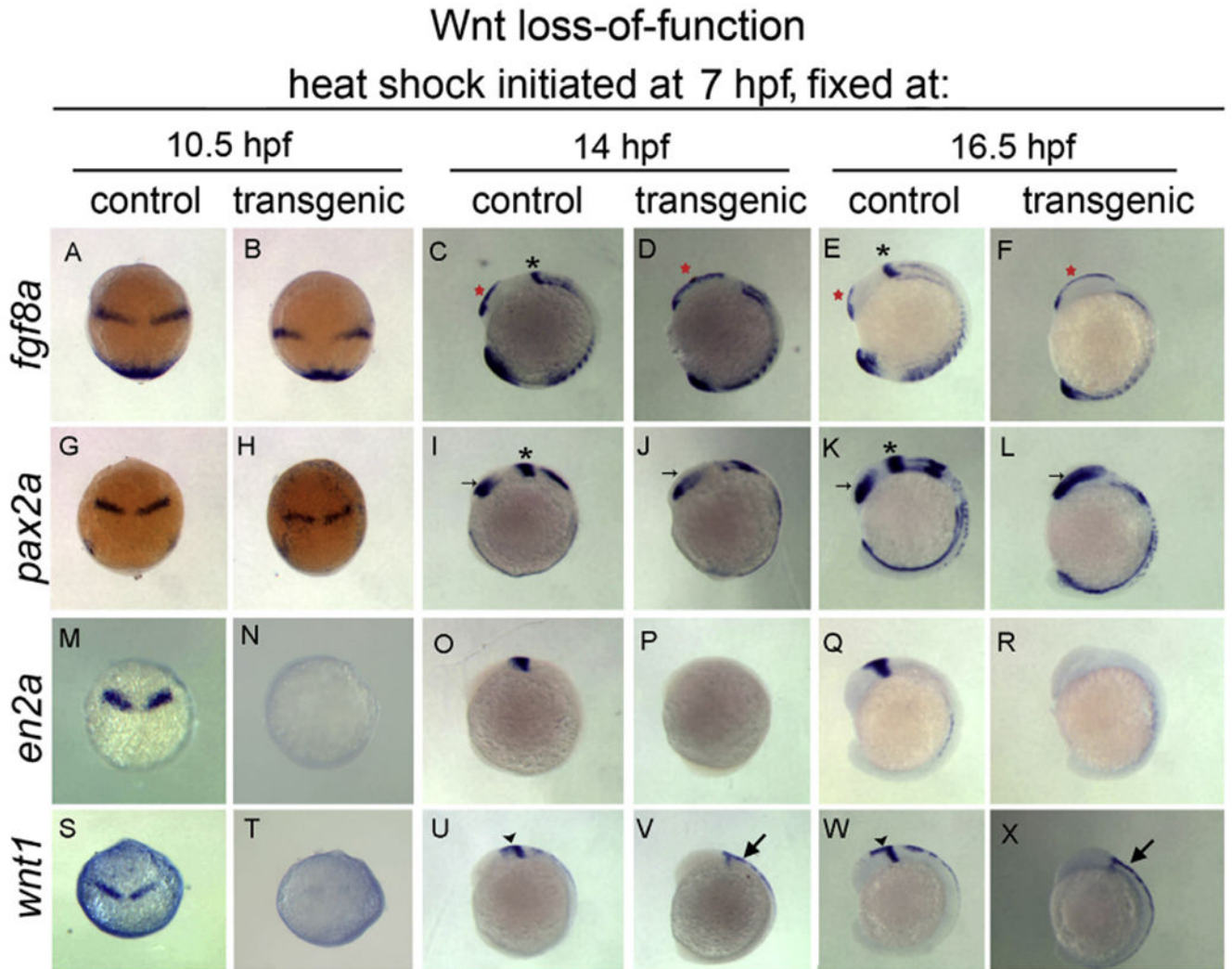


**Fig. 3. Wnt suppression during late epiboly/early segmentation leads to progressive loss of mes/r1 and expansion of forebrain.**

*In situ* hybridization to *fgf8a* (A–F), *pax2a* (G–L), *en2a* (M–R), and *wnt1* (S–X) on *hs:dkk1b*/+ or +/+ sibling embryos. Dorsal views, anterior up (A,B,G,H,M,N,S,T). Lateral views, dorsal right, anterior up (C–F, I-L, O-R, U-X). Note normal *fgf8a* and *pax2a* at 10.5 hpf, despite significant reduction of *wnt1* and *en2a*. By 14 hpf, MHB expression of *fgf8* and *pax2a* is lost (indicated by black asterisks, C,I,E,K absent in D,J,F,L) with posterior expansion of telencephalic *fgf8a* (red asterisks, C–F) and optic stalk *pax2a* (arrows, I-L). At 16 hpf, posterior expansion of forebrain has increased (E,F,K,L). Midbrain and MHB *wnt1* and *en2a* expression is absent, while dorsal hindbrain and spinal cord *wnt1* persists (large arrows, V,X).
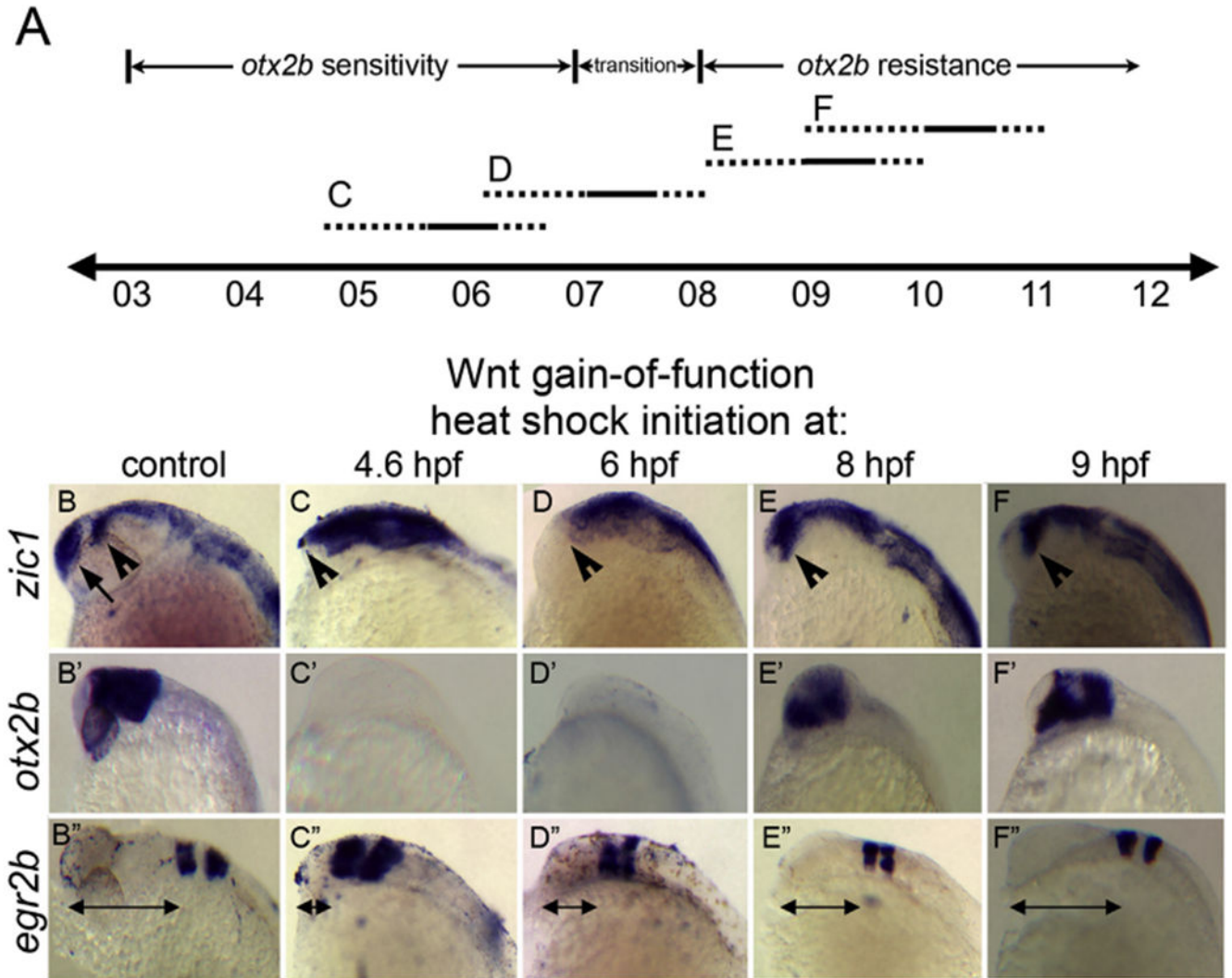
**Fig. 4. Timed global Wnt/β-catenin activation reveals two distinct windows of Wnt response.**
(A) Timeline (hours post fertilization) indicating periods of *hs:wnt8a* activation. Dashed lines represent uncertainty of beginning and end of Wnt pathway activation after heat shock. C,D,E,F: heat shock activation periods corresponding to images in bottom half of figure. (B–F") Lateral views of heads of 2427 hpf embryos, anterior left. (B–F) *In situ* hybridization to *zic1*. (B'-F') *otx2b*. (B"-F") *egr2b*. Control: +/+ siblings of *hs:wnt8a*/+ embryos. Note absence of telencephalic *zic1* domain (B, arrow) in all *hs:wnt8a*/+ embryos. Diencephalic *zic1* domain is absent after 4.6 and 6 hpf heat shocks (B,E,F, arrowheads). *otx2b* expression is suppressed after 4.6 and 6 hpf heat shocks but is present, but shifted anteriorly, after 8 hpf and 9 hpf heat shocks (C'-F'). *egr2b* expression within r3 and r5 are shifted anteriorly in all treatments with the degree of anterior shift decreasing with later heat shocks (B"-F", arrows).
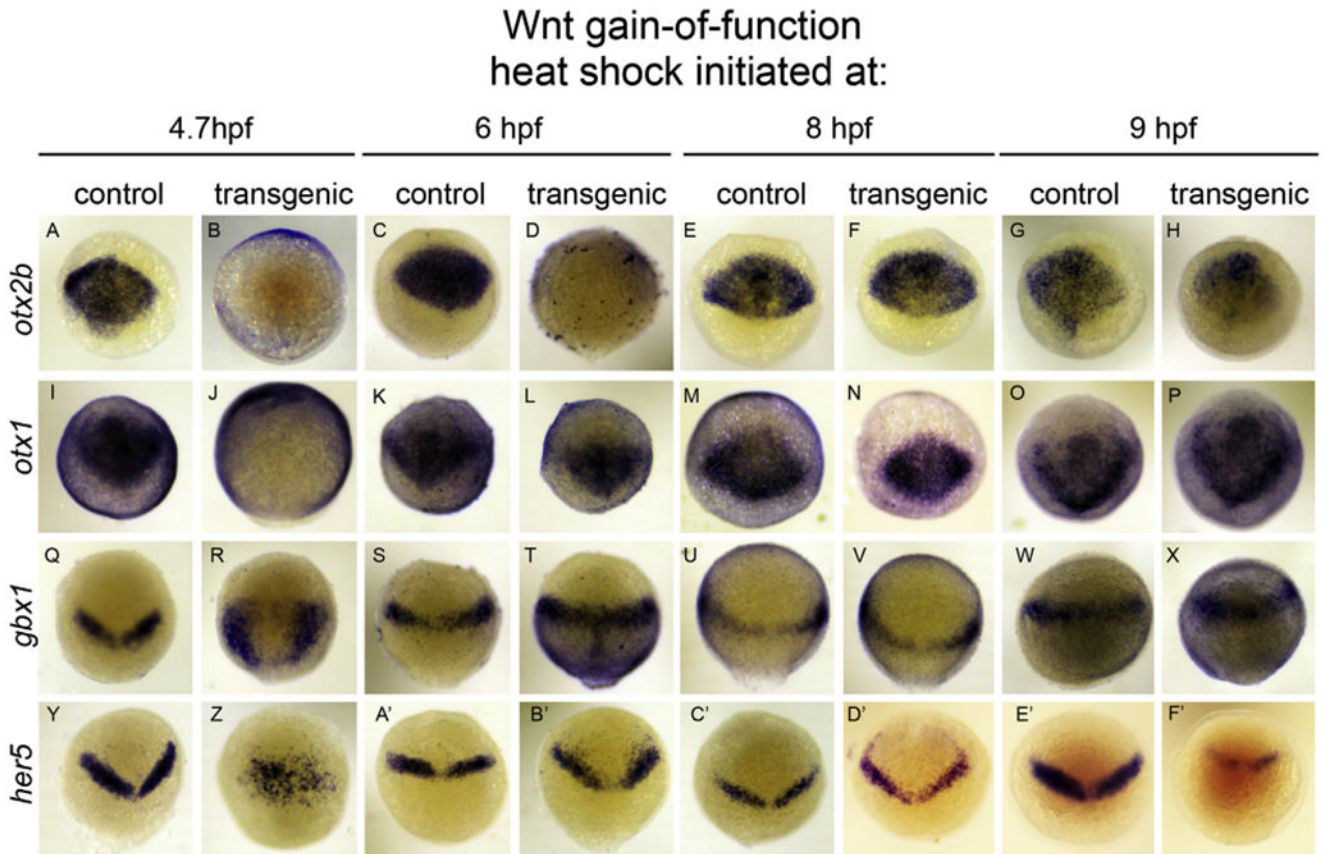
**Fig. 5. The neural plate responds dynamically to global Wnt activation during gastrulation.**
*In situ* hybridizations to *otx2b* (A–H), *otx1* (I–P), *gbx1* (Q–X), and *her5* (Y–F') on bud stage
*hs:wnt8a*/+ and +/+ sibling (control) embryos. Dorsal views, animal pole up. Time of heat
shock initiation is indicated above respective columns. Note repression of *otx2* (B) and *otx1*
(J) after 4.7 hpf heat shock, concomitant with anterior expansion of *gbx1* (R) and
disorganized *her5*+ cells (Z). *otx2b* repression occurs after 6 hpf heat shock (D), though *otx1*
does not (L), *gbx1* is mildly increased in the posterior neural plate (T), and *her5* shows
scattered expression anterior to normal domain (B'). Expression of all markers is relatively
normal after 8 hpf heat shocks (F,N,V) with slight anterior expansion of *her5* into
prospective telencephalic domain (D'). *otx2b, otx1* and *gbx1* are normal after 9 hpf heat
shock (H,P,X), while *her5* is reduced (F').
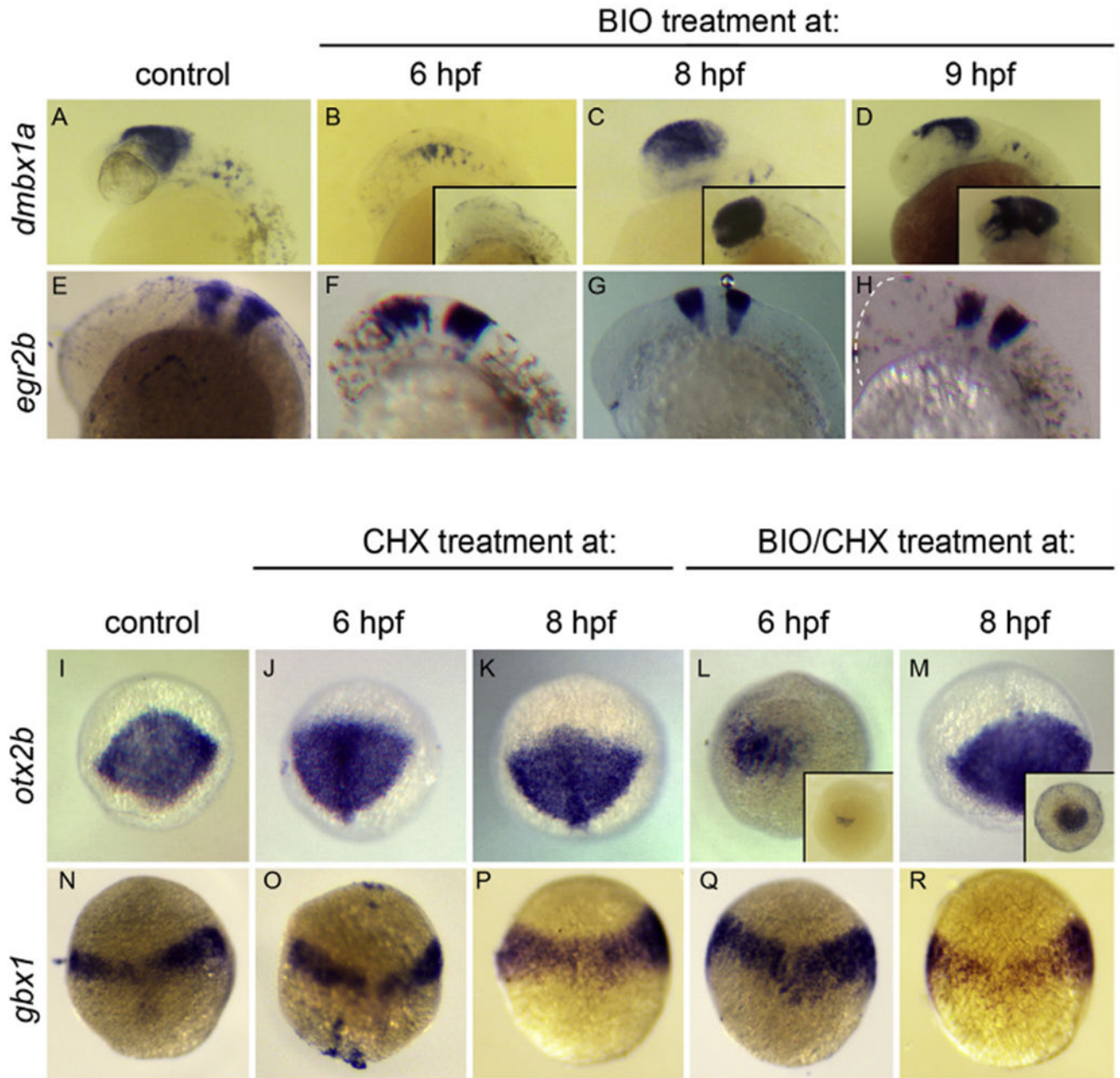
**Fig. 6. *otx2b* is directly suppressed by Wnt signaling.**
(A–H) BIO treatment recapitulates *hs:wnt8a* effects. *In situ* hybridization to *dmbx1a* in midbrain (A–D), *egr2b* in hindbrain (E–H). Insets in B,C,D show *otx2b* staining. 27hpf embryos anterior left, dorsal up. Note suppression of midbrain *dmbx1a* and *otx2b* after BIO treatment at 6 hpf (B) that is not observed with 8 or 9 hpf treatment (C,D). *egr2b* is shifted anteriorly, with the degree of anterior shift correlated with time of treatment (E-H; dotted line indicates anterior edge of embryo in H). (I–R) BIO treatment suppresses *otx2b* in absence of new protein synthesis. Analysis of 10 hpf embryos, oblique dorsal views, animal pole up, in situ hybridizations to *otx2b* (I–M) or *gbx1* (N–R). (J,K,O,P) CHX treatment only. (L,M,Q,R) BIO + CHX treatment. Note the lack of neural plate *otx2b* after treatment with

BIO + CHX at 6 hpf (L), similar to treatment with BIO alone (inset in L), which is not observed after treatment at 8 hpf (M; inset: BIO alone). Remaining mesodermal *otx2b* positive cells are visible, though numbers vary between embryos. *gbx1* is not significantly affected with either CHX or CHX/BIO treatment (N–R).
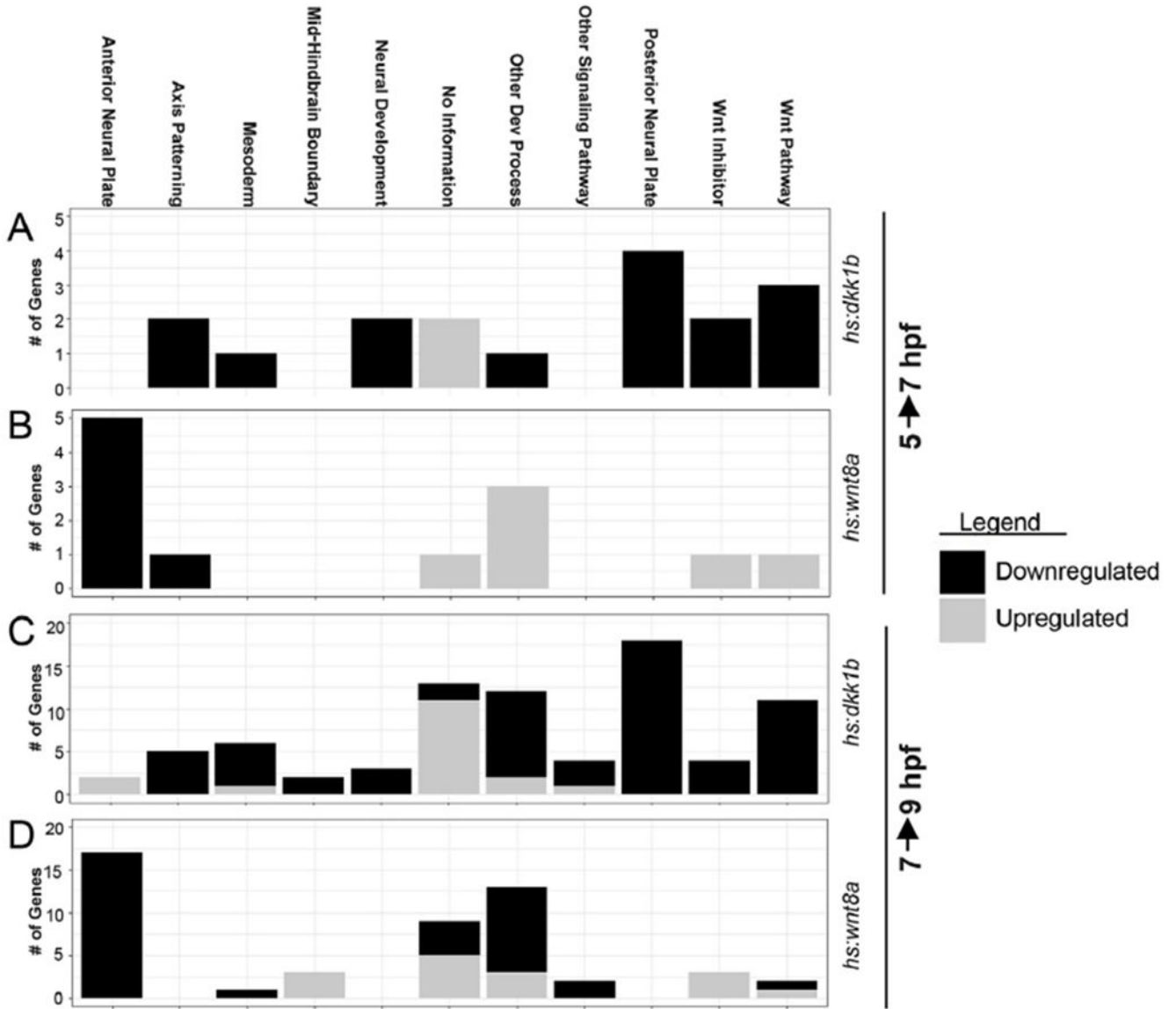
**Fig. 7. Functional classes of genes with significant transcriptional changes in response to Wnt pathway modulation during gastrulation.**
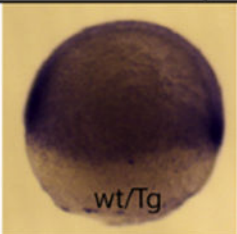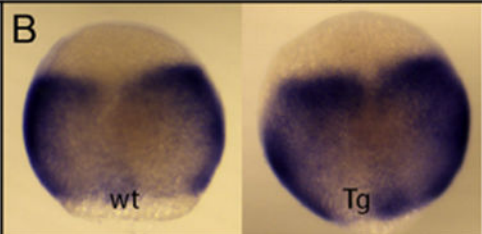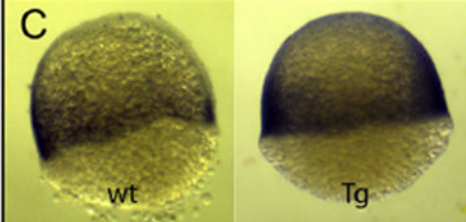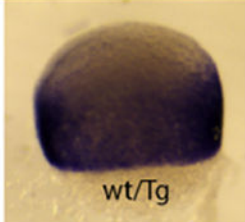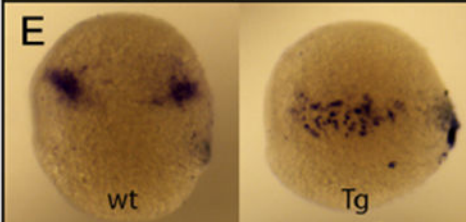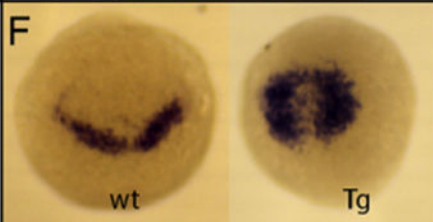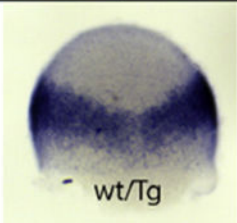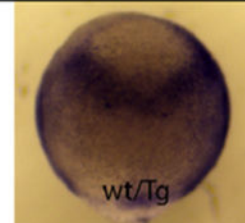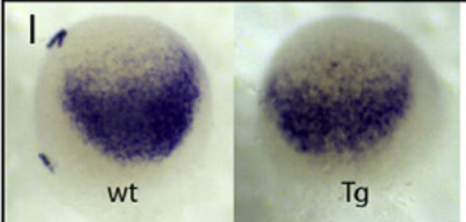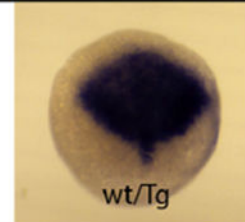
(A,B) Results from 5→7 hpf experiment. (C,D) Results from 7→9 hpf experiment. (A,C) Genes with significantly changed expression after induction of *hs:dkk1b*. (B,D) Genes with significantly changed expression after induction of *hs:wnt8a*. Genes were assigned categories based on functional and expression information obtained from the Zebrafish Information Network (ZFIN.org). Complete lists of genes can be found in Supplemental Tables 1–4.
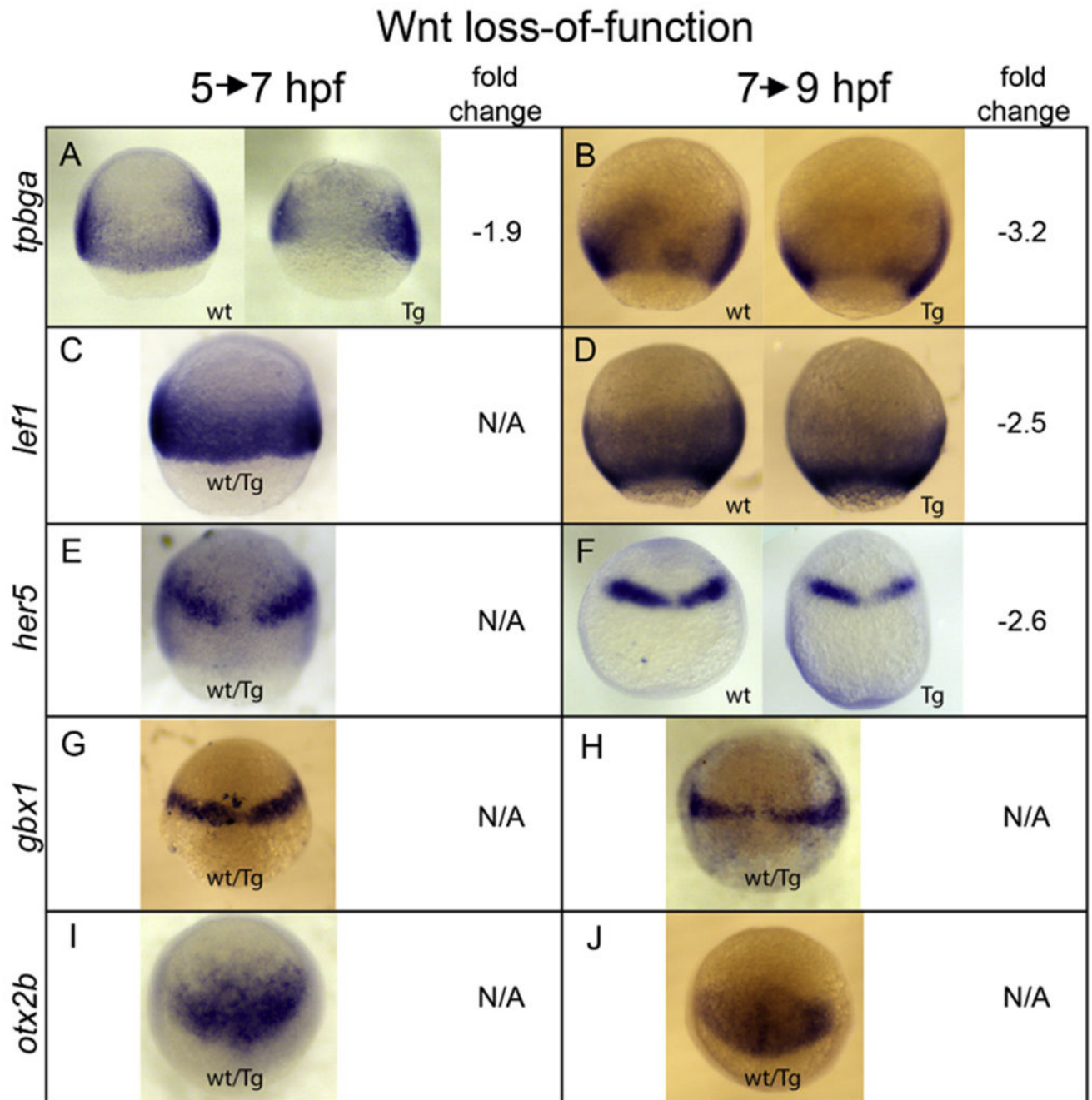
**Fig. 8. Validation of *hs:dkk1b* RNA-Seq analysis.**
Embryos collected from a *hs:dkk1b*/+ X +/+ cross were heat shocked during gastrulation according to experimental regimens outlined in Fig. S5 and fixed at 7 hpf (5→7 hpf experiment) or 9 hpf (7→9 hpf experiment) for in situ hybridization. Gene analyzed is indicated on left. Fold change is from the RNA-seq analysis (Supplemental Tables 1 and 2). wt: +/+ sibling. Tg: *hs:dkk1b*/+ embryo. wt/Tg: representative embryo from collection, genotype cannot be determined by staining pattern. Animal pole up, lateral views (A–D) or dorsal views (E–J).

**Fig. 9. Validation of *hs:wnt8a* RNA-Seq analysis.**
Embryos collected from a *hs:wnt8a*/+ X +/+ cross were heat shocked during gastrulation according to experimental regimens outlined in Fig. S5 and fixed at 7 hpf (5→7 hpf experiment) or 9 hpf (7→9 hpf experiment) for in situ hybridization. Gene analyzed is indicated on left. Fold change is from the RNA-seq analysis (Supplemental Tables 1 and 2). wt: +/+ sibling. Tg: *hs:dkk1b*/+ embryo. wt/Tg: representative embryo from collection, genotype cannot be determined by staining pattern. Animal pole up, lateral views (A,C,D) or dorsal views (B,E-J).
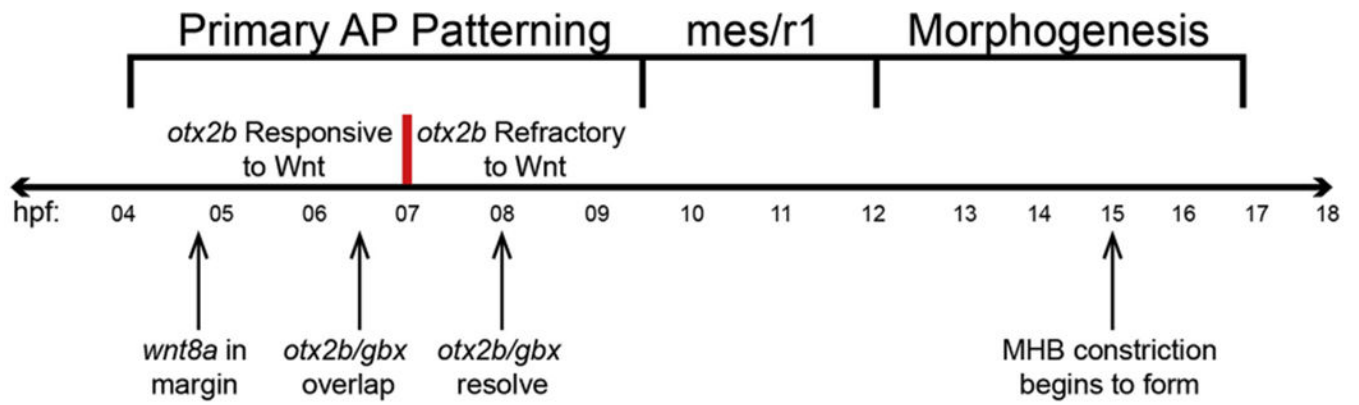
**Fig. 10. Model of temporal phases of Wnt-mediated neural patterning.**
Timeline of zebrafish development in hpf. Wnt-mediated neural patterning is divided into three phases; primary AP patterning, mes/R1, and morphogenesis. We overlay the dynamic competency of *otx2b* and the major developmental phases of the MHB.